Robust Statistical Enhancement Techniques for High-Density Impulse Noise Reduction

Arinjay Bhowmick, Rudrajit Choudhuri, Amiya Halder**

Department of Computer Science and Engineering,
St. Thomas' College of Engineering and Technology,
Kolkata, 700023, West Bengal, India.

*Corresponding author(s). E-mail(s): amiya.halder77@gmail.com;
Contributing authors: arinjaybhowmick@gmail.com;
rudrajit1729@gmail.com;

Abstract

Image quality enhancement via impulse noise reduction is a critical phase in image preprocessing. Faults in the acquisition, storage, and transmission devices often corrupt the images by introducing noise that further hinders image analysis and processing tasks. This paper focuses on high-density salt and pepper noise removal from images using statistical image enhancement techniques. We present two enhancement algorithms targeted at noise removal achieved through pixel regeneration. The first approach uses two-stage filtration based on an adaptive substructure; the noise is primarily eliminated using the non-noisy neighbors in an adaptive window, followed by fine-tuning the pixel intensity to remove artifacts. The second approach uses a quasi-adaptive substructure where the neighbors in primary directions contribute to the decision-making process of pixel regeneration based on their information relevance. Performance evaluation based on the inferences made from different experiments on multiple images verifies the efficiency of the presented techniques. The observed reliability and robustness reflected in the results suggest the superiority of the algorithms over their existing peers.

Keywords: High-Density Noise Removal, Statistical Enhancement Techniques, Salt and Pepper Noise

R. Murugan et al. (eds.), *Proceedings of the International Conference on Signal Processing and Computer Vision (SIPCOV 2023)*, Advances in Engineering Research 239,
https://doi.org/10.2991/978-94-6463-529-4_2

1 Introduction

Degradation of image quality often stems from the presence of corrupted image pixels. Relevant image details are lost when image pixels are replaced by noisy intensity values. The presence of noise hinders the performance of analysis and processing techniques including detection, classification, and segmentation among many others. Salt and pepper noise (SPN) is a common aberration category that corrupts an image by replacing pixel values with intensities at extreme ends of the spectrum. The major causes behind SP noise corruption are malfunctioning devices (sensors, capture devices, storage devices) and faulty transmission media.

Image enhancement achieved via noise reduction is a crucial preprocessing step often incorporated in image analysis pipelines to maintain relevant image details. The domain is fairly explored and various techniques have been designed to tackle the degradation problem induced by the presence of noise. Initial statistical approaches include the standard median filters(SMF) [1] and the fuzzy logic incorporated modified median filter FIDT [2]. Notable successors to these approaches are the selective adaptive median filter (SAMF) [4], sequentially combined mean-median filter (SCMMF) [3], and the modified median filter (MDMF) [5]. Several other algorithms have been published over the decades [9],[10],[8],[11],[12],[14],[13],[6]. These algorithms work fairly well for medium noise densities, but their resiliency drops at higher corruption levels. Recent advancements in the domain[15],[7],[16] effectively reduce noise from images, but for high corruption levels, the output image is induced with artifacts.

To tackle the drawbacks in literature and to improve upon the performance of the cutting edge methods, we propose two statistical enhancement approaches targeted at high-density salt and pepper noise removal from images. The first algorithm incorporates two-stage noise adaptive filtration where initially an intermediate image is formed using the available input image details and is further fine-tuned to get rid of the artifacts. The second method uses an quasi-adaptive paragon and incorporates data points in pixel regeneration based on their spatial relevance. The performance of the existing algorithms along with the presented techniques are evaluated using multiple images. Qualitative and quantitative inferences confirm the reliability and resiliency of the proposed algorithms.

The main contributions of the paper are:

1. A statistical two stage noise adaptive filter (STSNAF) is proposed.
2. A quasi-adaptive distance based weighted average filter (QADWAF) is proposed.
3. Quantitative inferences are analyzed to study the performances of the existing techniques compared with the presented algorithms.

The rest of the paper structure is organized as follows: Section 2 discusses the related work in literature. The proposed techniques are detailed in Section 3, Section 4 analyzes the experimental results, and finally conclusion is derived in Section 5.

2 Related Work

The domain of pixel regeneration, noise reduction, and image enhancement is quite popular in the field of image processing. Over the years, researchers have presented different methods and filtering techniques focused on noise elimination from images.

Standard median filter (SMF) [1] is one of the initial filtering techniques incorporated for SP noise removal. The incorporation of fuzzy logic with median filtering resulted in the FIDT [2] algorithm where a linear combination of fuzziness factor and neighborhood median is used to replace noisy pixels. Other algorithms such as a sequentially combined mean median filter (SCMMF) [3], selective adaptive median filter (SAMF) [4], total variation inpainting filter (TVIF) [19], and modified median filter (MDMF) [5] also laid foundation stones in the domain. The use of information sets in pixel regeneration came into picture with the proposal of noise adaptive information set based switching median (NAISM) [15] filtering approach. These techniques are efficient for mid-range noise densities but their performance drops significantly for higher density noise corruptions. Noise removal based on the use of directional weighted filters [18] and compressed sensing [20] have pushed the knowledge boundary in the domain of image enhancement. In 2015, Pilevar proposed a filtration technique for noise removal in color images [21] incorporating laplacian operators and thresholding criterion.

Recent developments in the field include an improved pixel density based filtration (IBPDF) [6], adaptive switching modified decision-based unsymmetric trimmed median filter (ASMDBUTMF) [7], modified decision based unsymmetric adaptive neighborhood trimmed mean filter (MDBUANTMF) [16], asymmetric trimmed trimean filter [24], feedback median filter [25], and statistical detail aware based filter [26]. These algorithms perform better than their peers but the regenerated images succumb to artifacts and loss of fine details is observed for high density noise reduction. Also, some of the mentioned approaches come with a huge time complexity trade off which raises issues in real time integration.

3 Proposed Methodology

In this section, we present two statistical enhancement techniques targeted at salt and pepper noise removal from images. The first approach uses two-stage filtration where an intermediate image is generated based on available image details and is further fine-tuned to remove unwanted aberrations. The second algorithm is based on a quasi-adaptive substructure where decision-making for pixel regeneration is based on the pixel relevance of non-noisy neighbors.

Prior to image enhancement, appropriate padding is applied on each side of the image (I). The noisy pixels are at extreme ends of the intensity spectrum (Pepper Noise: $INT_{min} = 0$ and Salt Noise: $INT_{max} = 255$) in a salt and pepper noise corrupted image. For denoting the noisy and noise-free pixels, a binary map G is constructed having the same dimensions as the image. The mapping is governed by the function defined in Eqn. 1. The binary map is then used in the presented enhancement algorithms for locating noisy pixels.

$$G_{i,j} = \begin{cases} 0, \text{ if } I_{i,j} = 0 \text{ or } 255. \\ 1, \text{ otherwise.} \end{cases} \quad (1)$$

Once the mapping is complete, i.e. the corrupted pixels in the image are detected, the algorithms are ready to be executed.

3.1 Proposed Algorithm 1: Statistical Two Stage Noise Adaptive Filter (STSNAF)

This subsection details a statistical two-stage noise adaptive filtration technique focused at restoring images corrupted by salt and pepper noise. Stage 1 incorporates adaptive median filtering for each noisy pixel $I_{i,j}$ (corresponding $G_{i,j} = 0$). Initially, a 3×3 window around the pixel (i, j) is selected. The window size is adaptively increased till non-noisy neighbors are found, or the maximum window size (W_{max}) is reached. If relevant pixels are found, the corrupted pixel is replaced by the median of its non-noisy neighbors. If not then the pixel is not updated. Stage 1 ensures that there is relevant image detail in the intermediate image before passing it to the next stage.

Stage 2 focuses on fine-tuning the pixels replaced in Stage 1. Initially, for each pixel at co-ordinate (i, j) [corresponding $G_{i,j} = 0$], a pixel relevance measure(ξ) (presented in the paper) of its immediate relevant neighbors are calculated using Eqn. 2.

$$\xi_{m,n} = \frac{e^{\left(\frac{-(m^2+n^2)}{\phi}\right)}}{8\pi} \quad (2)$$

where m, n are the spatial co-ordinates of the immediate neighbors around the image pixel (i, j) and ϕ is a control parameter. Finally, the output pixel ($I^{/}_{(i,j)}$) is computed using Eqn. 3 (incorporating the idea of weighted average).

$$I^{/}_{(i,j)} = \frac{\sum_{p=i-1,q=j-1}^{p=i+1,q=j+1} I_{p,q} * \xi_{p,q}}{\sum_{p=i-1,q=j-1}^{p=i+1,q=j+1} \xi_{p,q}} \quad (3)$$

The proposed STSNAF algorithm is summarized in Algorithm 1.

3.2 Proposed Algorithm 2: Quasi-Adaptive Distance based Weighted Average Filter (QADWAF)

A novel quasi adaptive distance relevant weighted average filtering technique is detailed in this section. The algorithm parses the image sequentially and on finding a noisy pixel (corresponding $G(i, j) = 0$), it looks for non-noisy neighboring pixels in every primary direction (left, right, up, down). Each direction is independent of the others, enabling locating pixels easier than using an adaptive window to find credible neighbors with local information. Next, the taxicab distance between the central pixel and the located neighbors are calculated. The distance metric is inversed and is used as a distance relevant weight as shown in Eqn. 4 which defines the considerable degree of information to be considered from each located neighbor. The idea reduces artifacts in the image as a far off pixel is assigned a much lesser weight than a closer one, also assuring that

Algorithm 1: STATISTICAL TWO STAGE NOISE ADAPTIVE FILTER (STSNAF)

Input: Corrupted Image I of dimension $M \times N$
Output: Noise Reduced Enhanced Image $I^{/}$

Map the image to a binary matrix G where corrupted and noise free pixels are represented as 0 and 1 respectively.
Stage I filtration:
for $i = 1..M$ **do**
  for $j = 1..N$ **do**
    if $G_{i,j} = 0$ **then**
      Initialize $w = 1$, i.e. Window $(W) = (2w + 1) \times (2w + 1)$
      Compute the sum of elements in the window (W) centered at $G_{i,j}$
      if $sum = 0$ **then**
        Increase w by 1 and recompute the sum till $sum > 0$ or $W < W_{max}$.
      else
        Replace $I_{i,j}$ by the median of all non-noisy pixels in the window.

Stage II filtration: **for** $i = 1..M$ **do**
  for $j = 1..N$ **do**
    if $G_{i,j} = 0$ **then**
      Calculate relevance measure (ξ) for immediate neighbors using Eqn. 2.
      Compute the value of the output pixel $I^{/}_{(i,j)}$ using Eqn. 3.

the regenerated pixel will be computed using relevant local spatial information, and image structure (Eqn. 4).

$$R(i,j,i',j') = \frac{K}{|i - i'| + |j - j'|} \tag{4}$$

where (i', j') represent the neighborhood pixel coordinate, and K is a scaling factor. After locating the pixels in each direction and assigning weights to each of them based on their distance, a weighted average is calculated corresponding to the central pixel using Eqn. 5. Next, the output image pixel intensity value is generated governed by Eqn. 6. The proposed technique is summarized in Algorithm 2.

$$\phi_{i,j} = \frac{\sum I_{i,j} * R(i,j,i',j')}{\sum R(i,j,i',j')} \tag{5}$$

$$I^{/}_{(i,j)} = \begin{cases} \phi_{i,j}, & \text{if } G(i,j) = 0 \text{ and } \sum R(i,j,i',j') > 0. \\ I_{i,j}, & \text{otherwise.} \end{cases} \tag{6}$$

Algorithm 2: Quasi-Adaptive Distance based Weighted Average Filter (QADWAF)

Input: Salt and Pepper Corrupted Image (I); dimensions $M \times N$.
Output: Noise Reduced Image I'.

Map the input image to the binary matrix G using Eqn. 1.
for $i = 1..M$ **do**
  for $j = 1..N$ **do**
    if $G_{i,j} = 0$ **then**
      Initialize $\phi - num_{i,j} = 0, \phi - den_{i,j} = 0$
      From the current pixel traverse upwards till boundary is reached, i.e. $i' = 0$ or till $G(i', j) = 1$
      if $G(i', j) = 1$ *and* $i' > 0$ **then**
        $\phi - num_{i,j} = \phi - num_{i,j} + I_{i,j} * R(i, j, i', j)$
        $\phi - den_{i,j} = \phi - den_{i,j} + R(i, j, i', j)$
      Similarly, traverse the left, right, and downward directions.
    Calculate $\phi_{i,j}$ and set the output pixel $I^{/}_{(i,j)}$ using Eqn. 6.

4 Experimental Result Analysis

This section analyzes the results obtained across various experiments in the context of the manuscript. First, the data source and the experimental setup are highlighted. Next, the performance metrics used for algorithmic evaluation is summarized. Finally, the performances are analyzed and the inferences are reported.

4.1 Data and Experimental Setup

For performance comparison, high quality standard gray scale images (Airplane, Barbara, Boat, Cameraman, House, Kiel, Mandril, Pepper, Zelda) [27] [28] are obtained. Each of these images are corrupted with SP noise with densities varying from as low as 40% to as high as 95%.

For all experiments, the maximum window size is set to 13×13. All experiments are performed under a Windows 10 Operating System with Intel i5 8th generation processor and 8GB RAM. Dev C++ served as the implementation platform.

4.2 Quantitatve Evaluation Metrics

Quantitative metrics are relevant for evaluating the efficiency of a processing technique. In this paper, we use four quantitative metrics, namely: Peak Signal to Noise Ratio (PSNR), Structural Similarity Measure (SSIM), Root Mean Squared Error (RMSE), and Image Enhancement Factor (IEF) (See Eqns. 7-10). RMSE measures the deviation between the original and the reconstructed image, thus highlighting any flaws in algorithmic resiliency. A low RMSE value signifies the efficiency of the enhancement technique. PSNR, IEF, and SSIM metrics evaluate the quality of the reconstructed image with respect to the original sample (high values represent robust performance of the processing technique).

$$PSNR(E_1, E_2) = 20log_{10}\frac{255}{RMSE} \tag{7}$$

$$RMSE(E_1, E_2) = \sqrt{(\frac{1}{P \times Q}\sum_{p=1}^{P}\sum_{q=1}^{Q}|E_1(p,q) - E_2(p,q)|^2)} \tag{8}$$

$$IEF(E_1, E_2, E_3) = \frac{\sum_{p=1}^{P}\sum_{q=1}^{Q}[E_1(p,q) - E_3(p,q)]^2}{\sum_{p=1}^{P}\sum_{q=1}^{Q}[E_1(p,q) - E_2(p,q)]^2} \tag{9}$$

$$SSIM = \frac{(2v_{E_1}v_{E_2} + b_1) + (2\nu_{E_1E_2} + b_2)}{(v_{E_1}^2 + v_{E_2}^2 + b_1) + (\nu_{E_1}^2 + \nu_{E_2}^2 + b_2)} \tag{10}$$

Here E_1 is the original, E_2 is the enhanced and E_3 represents the noisy image. The dimension of the image is $P \times Q$. v_{E_1}, v_{E_2} and ν_{E_1}, ν_{E_2} are the mean values and standard deviations of image E_1, E_2, respectively. $\nu_{E_1E_2}$ is the covariance of the images E_1 and E_2, b_1 and b_2 are the constants, and the value of $b_1 = (0.001 \times 255)^2$ and $b_2 = (0.03 \times 255)^2$.

4.3 Performance Evaluation

We compare the presented methods (STNAF and QADWAF) with the existing benchmark algorithms including SMF [1], SAMF[4], FIDT [2], SCMMF [3], MDMF [5], NAISM[15], IBPDF[6], ASMDBUTMF[7], and MDBUANTMF[16].

Tables 1-4 present the PSNR, RMSE, SSIM, IEF metrics corresponding to the Mandril image with noise densities varying from 40% to 95%. The RMSE values show a steep increasing trend with the increase in noise densities, particularly on and after 60%. The quality metrics on the other hand show a decreasing trend as high density corruption levels are reached. These observations demonstrate the flaws in algorithmic performance for high-density SP noise removal. The proposed methods, however, maintain a steady gradient representing better performance than its peers. Fig. 1 presents the enhanced Mandril output images corresponding to an 80% corrupted image. The visual indications defend the inferences drawn from Tables 1-4.

Similar inferences are drawn from Tables 5-8 corresponding to Pepper images. Visual results are presented in Fig. 2 and Fig. 3 for demonstrating the performance of the algorithms on Pepper and Barbara images.

Furthermore, for an extensive performance evaluation, experimentations were conducted on 25 different image sets, and the recorded average PSNR and SSIM values are presented in Tables 9- 10. The results are inline with the earlier observations and the metrics successfully defend the robustness of the proposed methods.

Table 1 PSNR values corresponding to different algorithms on `Mandril` image.

Noise Density	40	50	60	70	80	90	95
SMF	20.65	19.58	17.84	15.67	12.35	8.86	7.08
FIDT	22.04	21.02	19.66	17.77	14.63	10.69	8.14
SCMMF	25.8	24.53	23.12	21.47	19.34	17.04	16.11
SAMF	23.89	22.47	21.13	19.99	18.78	17.33	15.7
MDMF	25.25	23.92	22.43	20.72	18.39	15.62	14.13
NAISM	25.06	23.71	22.5	21.33	20.09	18.24	15.76
IBPDF	25.26	24.02	22.78	21.67	20.46	18.52	14.13
ASMDBUTMF	25.03	23.69	22.43	21.27	20.1	18.56	16.74
MDBUANTMF	25.03	23.69	22.43	21.27	20.09	18.6	16.73
STNAF	25	23.71	22.59	21.35	19.97	18.93	18.56
QADWAF	26.33	25.01	23.76	22.69	21.54	20.33	19.51

Table 2 RMSE values corresponding to different algorithms on `Mandril` image.

Noise Density	40	50	60	70	80	90	95
SMF	23.67	26.75	32.69	41.96	61.5	91.96	112.87
FIDT	20.17	22.68	26.53	32.97	47.33	74.44	99.89
SCMMF	13.08	15.14	17.8	21.52	27.52	35.84	39.92
SAMF	16.3	19.18	22.39	25.52	29.35	34.66	41.82
MDMF	13.93	16.24	19.28	23.47	30.7	42.21	50.11
NAISM	14.25	16.63	19.13	21.88	25.25	31.24	41.53
IBPDF	13.92	16.06	18.52	21.04	24.19	30.25	50.11
ASMDBUTMF	14.28	16.67	19.27	22.03	25.22	30.09	37.13
MDBUANTMF	14.28	16.67	19.28	22.03	25.24	29.96	37.15
STNAF	12.32	14.35	16.63	18.93	21.84	25.6	28.86
QADWAF	12.3	14.32	16.55	18.72	21.36	24.54	26.97

Table 3 SSIM values corresponding to different algorithms on `Mandril` image.

Noise Density	40	50	60	70	80	90	95
SMF	0.8304	0.7873	0.7051	0.5737	0.3474	0.1404	0.0651
FIDT	0.888	0.8586	0.8107	0.7256	0.5323	0.2614	0.116
SCMMF	0.9509	0.9331	0.9055	0.8554	0.7389	0.4683	0.2577
SAMF	0.926	0.8974	0.8607	0.82	0.7622	0.678	0.5695
MDMF	0.9451	0.925	0.8942	0.8434	0.7337	0.5064	0.3087
NAISM	0.9421	0.92	0.8925	0.8564	0.8017	0.673	0.3634
IBPDF	0.9452	0.9267	0.9023	0.8738	0.833	0.7478	0.4987
ASMDBUTMF	0.9418	0.9196	0.8913	0.8554	0.8039	0.7021	0.4968
MDBUANTMF	0.9418	0.9196	0.8913	0.8554	0.8036	0.7047	0.5023
STNAF	0.9562	0.9397	0.9177	0.8914	0.8516	0.7894	0.7205
QADWAF	0.9563	0.9397	0.9181	0.8931	0.8566	0.8036	0.75in1

5 Conclusion

Two different statistical enhancement methods are presented in the manuscript. Quantitative and qualitative inferences made from different experiments defend the reliability of the approach and establish the robustness of the techniques over the existing methods. The methods are simple to implement and can be easily integrated with embedded systems for direct enhancement. The algorithms can be scaled to have

Table 4 IEF values corresponding to different algorithms on `Mandril` image.

Noise Density	40	50	60	70	80	90	95
SMF	12.9	12.68	10.15	7.19	3.82	1.92	1.35
FIDT	17.77	17.64	15.41	11.64	6.45	2.93	1.72
SCMMF	43.66	40.74	35.33	28.15	19.64	13.05	11.1
SAMF	27.19	24.68	21.62	19.43	16.78	13.52	9.81
MDMF	37.21	34.4	29.17	22.98	15.34	9.12	6.84
NAISM	35.6	32.83	29.63	26.43	22.68	16.64	9.95
IBPDF	37.28	35.19	31.63	28.58	24.71	17.76	6.83
ASMDBUTMF	35.41	32.65	29.19	26.07	22.73	17.94	12.45
MDBUANTMF	35.41	32.65	29.18	26.07	22.69	18.1	12.44
STNAF	47.62	44.09	39.19	35.31	30.3	24.8	20.61
QADWAF	47.75	44.24	39.6	36.12	31.69	26.99	23.6

Table 5 Comparing PSNR values of enhanced `Pepper` images using different methods.

Noise Density	40	50	60	70	80	90	95
SMF	26.46	23.64	20.12	16.38	12.56	8.73	6.93
FIDT	27.3	25.78	23.51	20.05	15.59	10.89	8.3
SCMMF	34.79	32.87	29.67	24.42	19.43	15.53	14.23
SAMF	31.68	30.13	28.4	26.64	24.75	21.94	18.79
MDMF	33.69	31.44	28.33	24.06	19.54	15.32	13.35
NAISM	33.57	31.69	29.5	26.97	23.56	18.16	14.01
IBPDF	33.9	32.46	31.13	29.79	28.17	23.79	15.98
ASMDBUTMF	33.55	31.63	29.41	26.96	23.73	19	15.55
MDBUANTMF	33.55	31.62	29.4	26.96	23.73	19.03	15.56
STNAF	34.76	33.32	31.78	29.97	27.58	23.7	20.61
QADWAF	34.91	33.51	32.19	30.58	28.79	25.75	23.27

Table 6 Comparing RMSE values of enhanced `Pepper` images using different methods.

Noise Density	40	50	60	70	80	90	95
SMF	12.11	16.76	25.13	38.66	60.01	93.29	114.74
FIDT	11	13.1	17.01	25.34	42.33	72.76	97.96
SCMMF	4.64	5.79	8.38	15.33	27.22	42.69	49.53
SAMF	6.64	7.95	9.69	11.87	14.75	20.4	29.31
MDMF	5.27	6.83	9.77	15.97	26.9	43.71	54.85
NAISM	5.35	6.64	8.54	11.43	16.93	31.52	50.8
IBPDF	5.15	6.07	7.08	8.26	9.95	16.48	40.51
ASMDBUTMF	5.36	6.69	8.63	11.44	16.59	28.61	42.58
MDBUANTMF	5.36	6.69	8.64	11.45	16.6	28.52	42.54
STNAF	4.66	5.5	6.57	8.09	10.66	16.66	23.78
QADWAF	4.58	5.38	6.26	7.54	9.27	13.15	17.5

applications in the medical domain where corrupted medical images owing to faults in acquisition can be enhanced in real time.

Table 7 Comparing SSIM values of enhanced `Pepper` images using different methods.

Noise Density	40	50	60	70	80	90	95
SMF	0.9746	0.9518	0.8948	0.7716	0.5482	0.2594	0.1203
FIDT	0.9793	0.9708	0.9516	0.8972	0.7463	0.4516	0.2441
SCMMF	0.9963	0.9942	0.9877	0.9574	0.8525	0.5471	0.2832
SAMF	0.9924	0.9892	0.9839	0.9758	0.9627	0.929	0.8592
MDMF	0.9952	0.992	0.9835	0.9557	0.8726	0.6491	0.4233
NAISM	0.9951	0.9924	0.9874	0.9773	0.9497	0.8155	0.4533
IBPDF	0.9954	0.9937	0.9914	0.9882	0.9829	0.9537	0.7634
ASMDBUTMF	0.9951	0.9923	0.9871	0.9773	0.9518	0.8486	0.618
MDBUANTMF	0.9951	0.9923	0.9871	0.9773	0.9518	0.8495	0.6197
STNAF	0.9962	0.9948	0.9925	0.9885	0.9799	0.9495	0.8925
QADWAF	0.9964	0.995	0.9932	0.99	0.9847	0.968	0.9405

Table 8 Comparing IEF values of enhanced `Pepper` images using different methods.

Noise Density	40	50	60	70	80	90	95
SMF	52.59	34.28	18.29	9.02	4.28	1.98	1.38
FIDT	63.73	56.14	39.9	20.99	8.6	3.26	1.89
SCMMF	308.74	246.92	141.9	49.39	17.89	8.18	6.41
SAMF	174.72	152.58	123.05	95.69	70.92	41.59	21.2
MDMF	277.55	206.55	121	52.9	21.33	9.06	6.05
NAISM	269.93	218.64	158.6	103.34	53.81	17.42	7.06
IBPDF	290.95	261.33	230.63	197.79	155.88	63.75	11.1
ASMDBUTMF	268.41	215.44	155.11	103.07	56.04	21.14	10.05
MDBUANTMF	268.43	215.34	154.95	103.01	55.98	21.27	10.06
STNAF	354.93	318.61	267.92	206.06	135.9	62.36	32.19
QADWAF	367.76	332.85	294.59	237.11	179.68	100.03	59.48

Table 9 Average PSNR values (obtained using 25 standard gray-scale images) corresponding to different methods.

Noise Density	40	50	60	70	80	90	95
SMF	24.11	21.98	19.21	16.01	12.4	8.63	6.78
FIDT	25.07	23.85	22	19.16	15.31	10.75in	8.08
SCMMF	31.34	29.63	27.08	23.45	19.43	16	14.76
SAMF	28.45	26.92	25.4	23.9	22.31	19.99	17.3
MDMF	30.32	28.42	25.82	22.5	18.7	14.87	12.99
NAISM	30.14	28.37	26.61	24.58	22.24	18.15	14.68
IBPDF	30.47	29.03	27.7	26.35	24.93	21.62	15.16
ASMDBUTMF	30.13	28.35	26.57	24.6	22.41	18.84	15.97
MDBUANTMF	30.13	28.35	26.58	24.6	22.4	18.84	15.96
STNAF	31.62	30.08	28.54	26.89	25.08	22.31	20.08
QADWAF	31.69	30.2	28.77	27.28	25.77	23.58	21.83

References

[1] Gonzalez,R.C. and Woods, R.E.: Digital Image processing, Prentice Hall, (2002).

[2] Wenbin Luo: Efficient removal of impulse noise from digital images. IEEE Transactions on Consumer Electronics, vol. 52, no. 2, pp. 523-527, (2006).

Table 10 Average SSIM values (obtained using 25 standard gray-scale images) corresponding to different methods.

Noise Density	40	50	60	70	80	90	95
SMF	0.9364	0.9061	0.8411	0.7116	0.4884	0.2155	0.0913
FIDT	0.9535	0.9396	0.9123	0.8467	0.687	0.3903	0.1962
SCMMF	0.985	0.9788	0.9662	0.9316	0.825	0.5369	0.2891
SAMF	0.9748	0.9647	0.9512	0.9339	0.9081	0.8557	0.7608
MDMF	0.9823	0.9744	0.9585	0.9208	0.8218	0.5883	0.3688
NAISM	0.9816	0.9736	0.9624	0.9439	0.909	0.7767	0.4575
IBPDF	0.9826	0.9764	0.9683	0.958	0.9432	0.8957	0.6752
ASMDBUTMF	0.9815	0.9735	0.9621	0.944	0.9124	0.8093	0.5989
MDBUANTMF	0.9815	0.9735	0.9621	0.9441	0.9123	0.8095	0.5991
STNAF	0.9864	0.981	0.9734	0.963	0.9464	0.9068	0.8476
QADWAF	0.9864	0.9812	0.9741	0.9648	0.9514	0.9244	0.8894

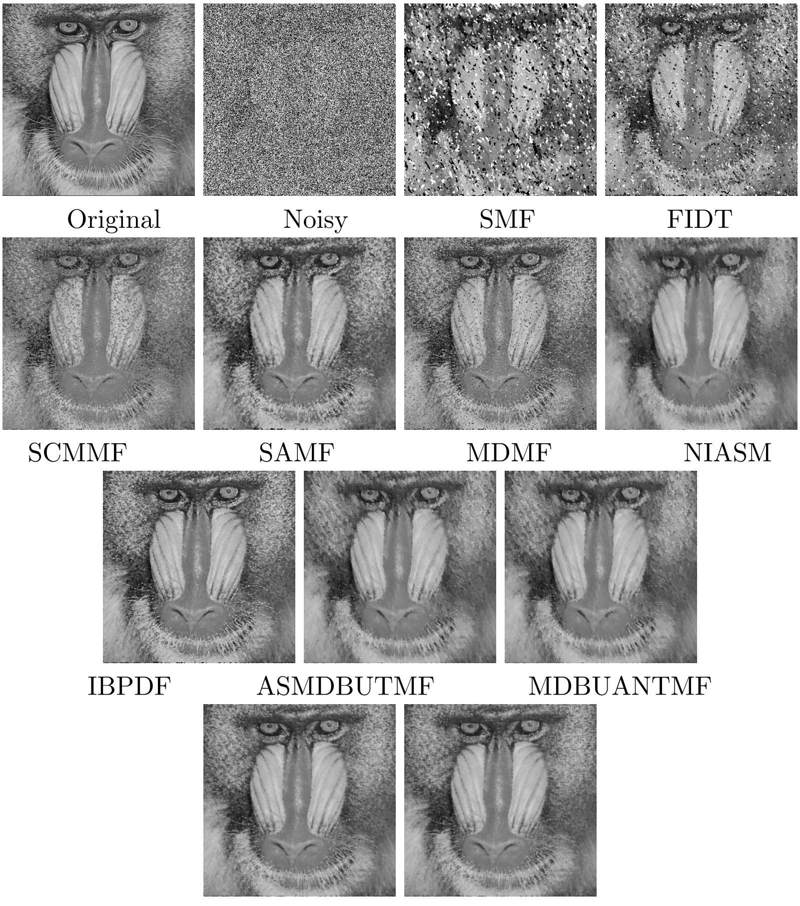

Fig. 1 Qualitative results corresponding to an 80% corrupted `Mandril` image.

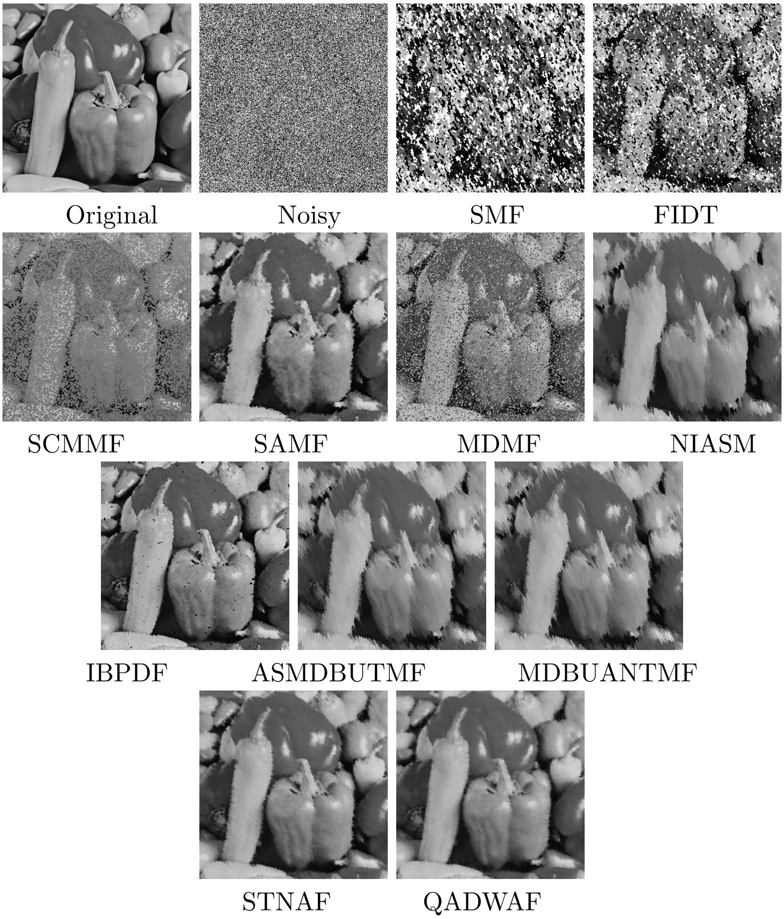

Fig. 2 Qualitative results corresponding to a 90% corrupted `Pepper` image.

[3] Banerjee, S and Bandyopadhyay, A and Bag, R and Das, A.: Sequentially combined mean-median filter for high density salt and pepper noise removal. 2015 IEEE International Conference on Research in Computational Intelligence and Communication Networks (ICRCICN), pp. 21-26 (2015).

[4] J. Das, B. Das, J. Saikia and S. R. Nirmala.: Removal of salt and pepper noise using selective adaptive median filter. International Conference on Accessibility to Digital World (ICADW), pp. 203-206, (2016).

[5] A. Soni and R. Shrivastava: Removal of high density salt and pepper noise removal by modified median filter. 2017 International Conference on Inventive Communication and Computational Technologies (ICICCT), Coimbatore, pp. 282-285, (2017).

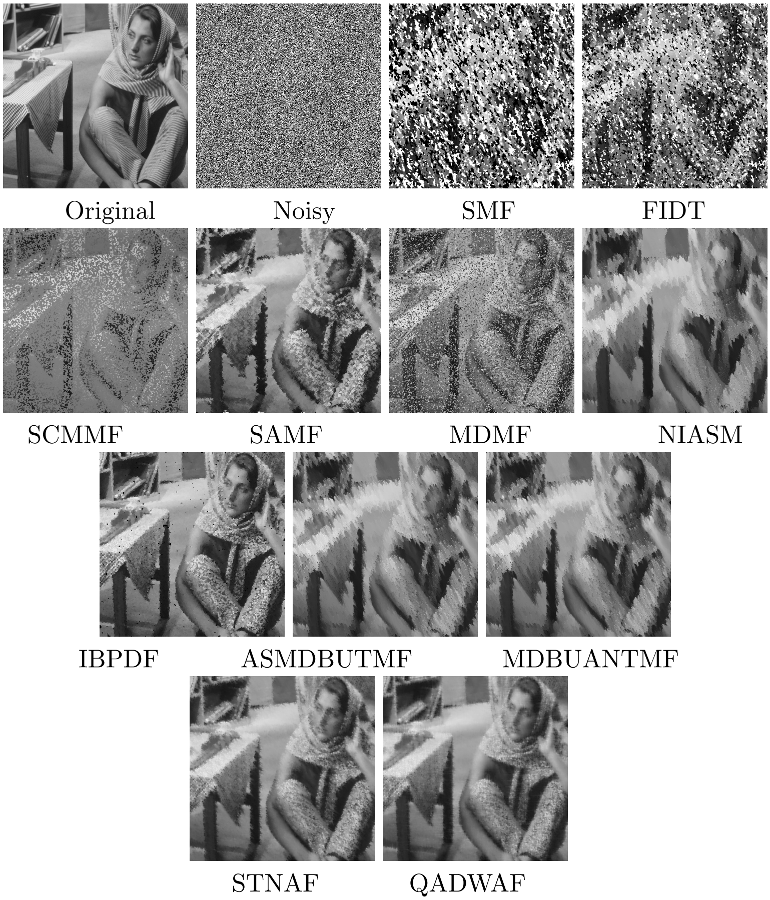

Fig. 3 Qualitative results corresponding to a 90% corrupted `Barbara` image.

[6] D. N. H. Thanh, L. Thi Thanh, V. B. Surya Prasath and U. Erkan. : An Improved BPDF Filter for High Density Salt and Pepper Denoising. 2019 IEEE-RIVF International Conference on Computing and Communication Technologies (RIVF), Danang, Vietnam, pp. 1-5,(2019).

[7] C. Jaspin Jeba Sheela, G. Suganthi.: An efficient denoising of impulse noise from MRI using adaptive switching modified decision based unsymmetric trimmed median filter. Biomedical Signal Processing and Control, 55, pp. 101657, (2020).

[8] Jayaraj V., Ebenezer D.: A new switching-based median filtering scheme and algorithm for removal of high-density salt and pepper noise in image. EURASIP journal on advances in signal processing, pp. 1-11, (2010).

[9] Zhang, S., Karim, M.A.: A new impulse detector for switching median filters. IEEE Signal Process. Lett. 9(11), 360-363 (2002).

[10] Ibrahim, H., Kong, N.S.P., Foo, T.F.: Simple adaptive median filter for the removal of impulse noise from highly corrupted images. IEEE Trans. Consum. Electron. 54(4), 1920-1927 (2008).

[11] Bhateja, V., Verma, A., Rastogi, K., Malhotra, C., Satapathy, S.C.: Performance improvement of decision median filter for suppression of salt and pepper noise. Adv. Intell. Syst. Comput. 264, 287-297 (2014).

[12] Halder A., Halder S. and Chakraborty, D. : A Novel Iterative Salt-and-Pepper Noise Removal Algorithm. Proceedings of the 4th International Conference on Frontiers in Intelligent Computing: Theory and Applications (FICTA), Springer, pp. 635-643, (2015).

[13] Erkan, U., Gokrem, L. and Enginoglu, S.: Different applied median fillter in salt-andpepper noise. Int. J. Comput. Electr. Eng. 70, 1-10 (2018).

[14] Chen,Q. Q. Hung, M. H., and Zou,F.: Effective and adaptive algorithm for pepper-andsalt noise removal. IET Image Process. 11(9), 709-716 (2017).

[15] Wang, Y. Han, L. Xiao, S. Wang, J. and Zhai, X : A nnovel statistical approach to remove salt-and-pepper noise, Journal of Statistical Computation and Simulation. 87(13), pp.2538–2548, (2017).

[16] Goel, Navdeep and Kaur, Harpreet and Saxena, Jyoti : Modified decision based unsymmetric adaptive neighborhood trimmed mean filter for removal of very high density salt and pepper noise, Multimedia Tools and Applications. 79(27), pp. 19739–19768, (2020).

[17] Wang, Xiaotian and Shen, Shanshan and Shi, Guangming and Xu, Yuannan and Zhang, Peiyu: Iterative non-local means filter for salt and pepper noise removal, Journal of visual communication and image representation. 38, pp. 440–450, (2016).

[18] Li, Zuoyong and Liu, Guanghai and Xu, Yong and Cheng, Yong: Modified directional weighted filter for removal of salt & pepper noise, Pattern Recognition Letters. 40, pp. 113–120, (2014).

[19] Wu, Jian and Tang, Chen: An efficient decision-based and edge-preserving method for salt-and-pepper noise removal, Pattern Recognition Letters. 32(15), 1974–1981, (2011).

[20] Huang, S and Zhu, J: Removal of salt-and-pepper noise based on compressed sensing, Electronics Letters. 46(17), pp. 1198–1199, (2010).

[21] Pilevar, Abdol Hamid and Saien, Soudeh and Khandel, Mina and Mansoori, Bahman: A new filter to remove salt and pepper noise in color images, Signal, Image and Video Processing. 9(4), pp. 779–786, (2015).

[22] Nasri, Mehdi and Saryazdi, Saeid and Nezamabadi-Pour, Hossein: A fast adaptive salt and pepper noise reduction method in images, Circuits, Systems, and Signal Processing. 32(4), pp. 1839–1857, (2013).

[23] Sulaiman, Siti Noraini and Isa, Nor Ashidi Mat: Denoising-based clustering algorithms for segmentation of low level salt-and-pepper noise-corrupted images, IEEE Transactions on Consumer Electronics. 56(4), pp. 2702–2710, (2010).

[24] Vasanth, K:A Decision Based Neighbourhood Referred Asymmetrically Trimmed Modified Trimean for the Removal of High Density Salt and Pepper Noise in Images and Videos, Wireless Personal Communications. pp.1–25, (2021).

[25] Maitra, Mausumi and Chakraborty, Susanta and others: A novel decision-based adaptive feedback median filter for high density impulse noise suppression, Multimedia Tools and Applications. 80(1), pp. 299–321, (2021).

[26] Liang, Hu and Li, Na and Zhao, Shengrong: Salt and Pepper Noise Removal Method Based on a Detail-Aware Filter, Symmetry. 13(3), pp. 515, (2021).

[27] http://sipi. usc. edu/database

[28] https://links.uwaterloo.ca/Repository.htm